Allosteric modulation by sodium ions and amilorides of G protein-coupled receptors : a closer look at the sodium ion site of the adenosine A2a receptor and development of a mass spectrometry ligand binding assay for adenosine A1 and A2a receptors

Massink, A.

Chapter 4

Sodium ion binding pocket mutations and adenosine A_{2A} receptor function

Arnault Massink*
Hugo Gutiérrez-de-Terán*
Eelke B. Lenselink
Natalia V. Ortiz Zacarías
Lizi Xia
Laura H. Heitman
Vsevolod Katritch
Raymond C. Stevens
Adriaan P. IJzerman

**These authors contributed equally*

Molecular Pharmacology, 2015, 87(2): 305-13

Abstract

Recently a sodium ion binding pocket in a high resolution structure of the human adenosine A_{2A} receptor was identified. In the present study we explored this binding site through site-directed mutagenesis and molecular dynamics simulations. Amino acids in the pocket were mutated to alanine, and their influence on agonist and antagonist affinity, allosterism by sodium ions and amilorides, and receptor functionality was explored. Mutation of the polar residues in the sodium ion pocket was shown to either abrogate (D52A$^{2.50}$ and N284A$^{7.49}$) or reduce (S91A$^{3.39}$, W246A$^{6.48}$, and N280A$^{7.45}$) the negative allosteric effect of sodium ions on agonist binding. Mutations D52A$^{2.50}$ and N284A$^{7.49}$ completely abolished receptor signaling, while mutations S91A$^{3.39}$ and N280A$^{7.45}$ elevated basal activity and mutations S91A$^{3.39}$, W246A$^{6.48}$, and N280A$^{7.45}$ decreased agonist-stimulated receptor signaling. In molecular dynamics simulations D52A$^{2.50}$ directly affected the mobility of sodium ions, which readily migrated to another pocket formed by Glu13$^{1.39}$ and His278$^{7.43}$. The D52A$^{2.50}$ mutation also decreased the potency of amiloride with respect to ligand displacement, but did not change orthosteric ligand affinity. In contrast, W246A$^{6.48}$ increased some of the allosteric effects of sodium ions and amiloride, while orthosteric ligand binding was decreased. These new findings suggest that the sodium ion in the allosteric binding pocket not only impacts ligand affinity, but also plays a vital role in receptor signaling. Because the sodium ion binding pocket is highly conserved in other class A GPCRs, our findings may have a general relevance for these receptors and may guide the design of novel synthetic allosteric modulators or bitopic ligands.

Introduction

G protein-coupled receptors (GPCRs) are seven transmembrane helical proteins, which regulate a multitude of physiological processes, and therefore are targeted by 30-40% of the drugs currently on the market.[1] GPCR crystal structures are becoming increasingly available, which considerably contributes to our understanding of both drug-receptor interactions and receptor activation mechanisms.[2] Still, much remains to be discovered and therefore the new crystal structure repertoire of GPCRs is continuously analyzed by biochemical, computational and pharmacological studies.

One of the most widely explored GPCRs is the human adenosine A_{2A} receptor ($hA_{2A}AR$), a drug target related to Parkinson's disease, cardiovascular diseases, and inflammatory disorders.[3] Recently, a high resolution crystal structure of the inactive $hA_{2A}AR$ in complex with antagonist ZM-241,385 identified the precise location of a sodium ion in the region around the conserved Asp52$^{2.50}$,[4] as previously hypothesized for other GPCRs[5, 6] (numbering in superscript according to Ballesteros and Weinstein).[7] Residues Ser91$^{3.39}$, Trp246$^{6.48}$, Asn280$^{7.45}$, and Asn284$^{7.49}$, together with a network of structural water molecules, completed the coordination of the ion in the $hA_{2A}AR$. The fact that this site changes its conformation dramatically between inactive and active-like structures of the $hA_{2A}AR$,[4, 8] inspired us to further explore the nature of this allosteric binding site.

In Chapter 3 we used a combination of molecular dynamics (MD) simulations, biophysical and biochemical experiments to conclude that sodium ions selectively stabilize the inactive conformation of the wild-type receptor, and that a physiological concentration was sufficient to achieve this effect. This mechanism was further corroborated with radioligand binding data, indicative of a competitive interaction between the sodium ion in this allosteric pocket and an agonist in the orthosteric pocket. Further, we proposed in Chapter 3 that the diuretic drug amiloride and analogs compete for the same site, and exert an allosteric control on the $hA_{2A}AR$ quite similar to that of sodium ions, albeit with pharmacological differences in modulation of orthosteric ligand binding.

In the present study we mutated residues in the first and second coordination shell around the sodium ion, to define the role of individual amino acids in allosteric modulation by sodium ions, amiloride and its derivative HMA. This enabled us to analyze

the effects of these manipulations on orthosteric ligand binding and receptor activation, employing a combination of biochemical and computational techniques.

Materials and methods

Cell growth and transfection

HEK293 cells were grown in culture medium consisting of Dulbecco's modified Eagle's medium (DMEM) supplemented with 10% newborn calf serum (NCS), 50 µg/ml streptomycin and 50 IU/ml penicillin at 37 °C and 7% CO_2. Cells were subcultured twice a week at a ratio of 1:20 on 10 cm ø plates. Single point mutations were introduced in the wild-type hA_{2A}AR-plasmid DNA (FLAG-tag at N-terminus, in pcDNA3.1) by BaseClear (Leiden, The Netherlands). Cells were transfected with the indicated plasmids (1 µg each) using the calcium phosphate precipitation method.[9] All experiments were performed 48 h after transfection. HEK293 cells stably expressing the wild-type A_{2A}AR receptor (A_{2A}AR-WT) were grown in the same medium as the other HEK293 cells but with the addition of G-418 (200 µg/ml).

Enzyme-linked immunosorbent assay

Twenty-four hours after transfection, cells were brought into 96-well poly-D-lysine-coated plates at a density of 10^5 cells per well. After an additional 24 h, the monolayers were washed with phosphate-buffered saline (PBS) and fixed for 10 minutes with 3.7% formaldehyde. Subsequently, cells were washed two times with PBS and cell-surface receptors were labeled with mouse anti-FLAG (M2) primary antibody (Sigma, 1:1000) in culture medium for 30 min at 37 °C. The cells were then washed once with DMEM supplemented with 25 mM HEPES and then incubated for another 30 min at 37 °C in culture medium supplemented with horseradish peroxidase-conjugated anti-mouse IgG produced in goat (Brunschwig, Amsterdam, The Netherlands; 1:5000) as the secondary antibody. The cells were washed twice with PBS. Finally, the cells were incubated with 3,3',5,5'-tetramethylbenzidine (TMB) for 5 min in the dark at room temperature. The reaction was stopped with 1 M H_3PO_4 and after 5 min the absorbance was read at 450 nm using a VICTOR 2 plate reader (PerkinElmer Life Sciences, Groningen, The Netherlands).

Radioligand binding assays

[^{3}H]ZM-241,385 (50 Ci/mmol) and [^{3}H]NECA (17 Ci/mmol) were obtained from ARC Inc. (St. Louis, MO, USA) and PerkinElmer (Groningen, The Netherlands), respectively. ZM-241,385 was obtained from Ascent Scientific (Bristol, UK). Amiloride and HMA were obtained from Sigma Aldrich (Zwijndrecht, The Netherlands). All other materials were purchased from commercial sources and were of the highest available purity.

HEK293 cells were grown and transfected as described above. Membranes were prepared as follows. Cells were detached from plates 48 h after transfection by scraping them into 5 ml PBS, collected and centrifuged at 700 ×g (3000 rpm) for 5 min. Pellets derived from 20 plates (10 cm ø) were pooled and resuspended in 16 ml of ice-cold assay buffer (50 mM Tris-HCl, pH 7.4). An Ultra-Turrax was used to homogenize the cell suspension. Membranes and the cytosolic fraction were separated by centrifugation at 100,000 ×g (31,000 rpm) in a Beckman Optima LE-80K ultracentrifuge (Woerden, The Netherlands) at 4 °C for 20 min. The pellet was resuspended in 8 ml of Tris buffer and the homogenization and centrifugation step was repeated. Assay buffer (4 ml) was used to resuspend the pellet and adenosine deaminase (ADA) was added (0.8 IU/ml) to break down endogenous adenosine. Membranes were stored in 250 µl aliquots at -80 °C. Membrane protein concentrations were measured using the BCA (bicinchoninic acid) method.[10]

For competition binding experiments with [^{3}H]ZM-241,385 membranes with transiently expressed A_{2A}AR-WT (7 µg of total protein), A_{2A}AR-D52A$^{2.50}$ (5 µg), A_{2A}AR-S91A$^{3.39}$ (1 µg), A_{2A}AR-W246A$^{6.48}$ (2 µg), A_{2A}AR-N280A$^{7.45}$ (1.5 µg), A_{2A}AR-N284A$^{7.49}$ (1 µg) were used; we added different protein amounts to ensure that total binding to the membrane preparations was less than 10% of the total radioactivity added in order to prevent radioligand depletion. For [^{3}H]NECA competition binding experiments 30 µg, 15 µg, 10 µg, 45 µg, 50 µg, 10 µg of expressed A_{2A}AR-WT, D52A$^{2.50}$, S91A$^{3.39}$, W246A$^{6.48}$, N280A$^{7.45}$, N284A$^{7.49}$ receptors were used, respectively. Membrane aliquots were incubated in a total volume of 100 µl of assay buffer at 25 °C for 2 h. For homologous competition curves, radioligand displacement experiments were performed in the presence of nine concentrations of NECA (0.1 nM – 100 µM) and ZM-241,385 (0.01 nM – 10 µM). For concentration-effect curves, radioligand displacement experiments were performed in the presence of six concentrations of NaCl (10 µM – 1 M) and five

concentrations of amiloride (100 nM – 1 mM) and HMA (10 nM – 1 mM). [^{3}H]ZM-241,385 and [^{3}H]NECA were used at concentrations of 2.5 nM and 20 nM, respectively. Nonspecific binding was determined in the presence of 10 μM ZM-241,385 ([^{3}H]NECA) or 100 μM NECA ([^{3}H]ZM-241,385) and represented less than 10% of the total binding. Incubations were terminated by rapid vacuum filtration to separate the bound from free radioligand through 96-well GF/B filter plates using a Filtermate-harvester (PerkinElmer Life Sciences). Filters were subsequently washed three times with ice-cold assay buffer. The filter-bound radioactivity was determined by scintillation spectrometry using a PE 1450 Microbeta Wallac Trilux scintillation counter (PerkinElmer Life Sciences).

Functional cAMP assays

HEK293 cells were grown and transfected as described above. Experiments were performed 48 h after transfection. The amount of cAMP produced was determined with the LANCE cAMP 384 kit (PerkinElmer). In short, 5000 cells per well were pre-incubated for 30 min at 37°C and subsequently incubated for one hour at room temperature with a range of CGS-21680 concentrations (0.1 nM – 10 μM), one concentration of ZM-241,385 (10 μM), or without addition of ligand. cAMP generation was performed in the medium containing cilostamide (50 μM), rolipram (50 μM) and ADA (0.8 IU·ml^{-1}). The incubation was stopped by adding detection mix and antibody solution, according to the instructions of the manufacturer. The generated fluorescence intensity was quantified on an EnVision® Multilabel Reader (PerkinElmer). cAMP production by 10 μM CGS-21680 on the parental HEK293 cell line represented less than 5% of cAMP production generated in cells expressing the hA_{2A}AR receptor.

Molecular dynamics simulations

Molecular dynamics (MD) simulations of wild-type and mutant forms of the A_{2A} receptor were performed following the computational protocol in Chapter 3. Briefly, the inactive structure of the A_{2A}AR in complex with ZM-241,385 and a sodium ion (PDB code 4EIY)[4] was used as a basis for our simulations, after a refinement process that consisted in modeling the missing ICL3 segment and proton addition, assessing the protonation state of titratable residues (i.e. all charged) and histidine residues, which were protonated on Nδ except for His155^{ECL2} (protonated on Nε) and His264^{ECL3} (positively charged). The sodium ion and coordinating water molecules were explicitly considered except in the simulations

with amiloride or HMA, which occupied the allosteric sodium ion site. Further details are summarized in Chapter 3. Building the mutant variants of the A_{2A} receptor explored in this work was achieved by means of the "protein mutation tool" in Maestro.[11]

MD simulations were performed with GROMACS software,[12] using our original protocol for the MD simulations of GPCRs.[13] Our PyMemDyn program was used for membrane insertion, soaking with bulk water and inserting the resulting system, consisting of approximately 50,000 atoms (~74% belong to solvent molecules, ~15% to lipids and ~11% to protein and ligand atoms), into a hexagonal prism-shaped box, which was then energy-minimized and carefully equilibrated in the framework of periodic boundary conditions (PBC) for 5 ns.[14] Three replicate production simulations (i.e., changing the initial velocities of the system) were followed for 100 ns simulation time each, thus accounting for a total of 300 ns MD sampling of each system. The OPLSAA force field was adopted throughout the simulations,[15] with ligand parameters obtained from Macromodel,[16] and lipid parameters adapted from Berger[17] together with the use of the half-ε double-pairlist method[18] and the SPC water model.[19] A Nose-Hoover thermostat[20] with a target temperature of 310 K was used. Electrostatic interactions beyond a cutoff of 12 Å were estimated with the particle mesh Ewald (PME) method. All MD analyses were conducted with several GROMACS and VMD[21] utilities. Molecular superimpositions, trajectory visualizations and molecular images were performed with PyMOL.[22]

Results

Design of mutations in the sodium ion binding pocket

We mutated the residues important for the sodium ion coordination (Figure 1) to alanine, i.e. D52A$^{2.50}$, S91A$^{3.39}$, W246A$^{6.48}$, N280A$^{7.45}$, and N284A$^{7.49}$. This approach thus yielded a total of five mutant receptors, which were studied further and compared to the wild-type receptor with respect to their expression levels and pharmacology.

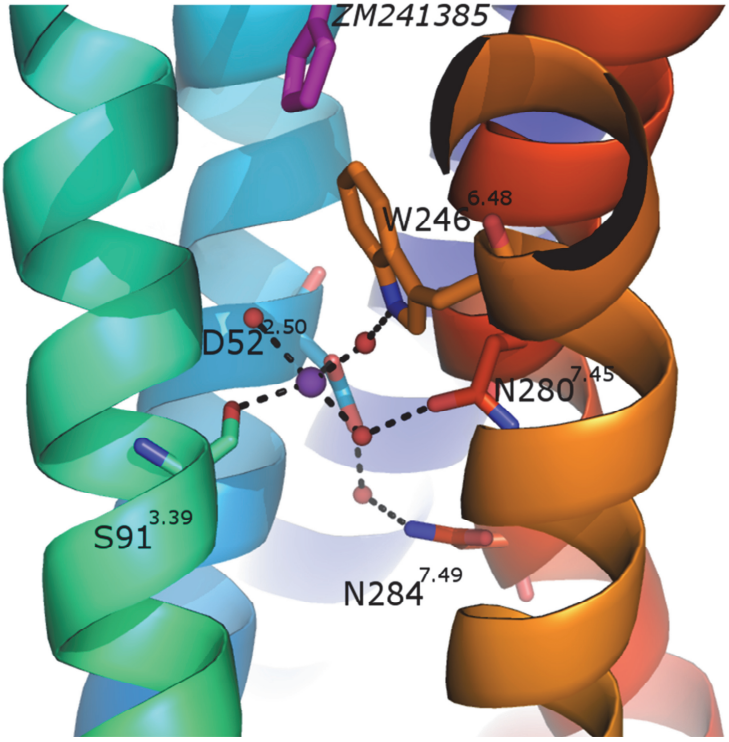

Figure 1. Residues in or close to the sodium ion binding site that we subjected to an alanine scan in the hA_{2A}AR, mapped on the crystal structure of the hA_{2A}AR in the inactive ZM-241,385 and sodium ion bound conformation (PDB 4EIY)[4]. Residues Asp52$^{2.50}$, Ser91$^{3.39}$, Trp246$^{6.48}$, Asn280$^{7.45}$, and Asn284$^{7.49}$ (represented by sticks, of which red and blue sticks are oxygen and nitrogen atoms, respectively) coordinate the sodium ion (purple sphere). Numbering of the residues follows the Ballesteros-Weinstein system for comparison of positions between GPCRs.[7] Water molecules interacting with the sodium ion are represented by red spheres; hydrogen bonds are represented by black dotted lines; receptor backbone is represented by ribbons. Purple stick structure on top represents (part of) co-crystallized ZM-241,385.

Cell surface receptor expression of mutated receptors

ELISA was performed on HEK293 cells transiently expressing FLAG-tagged wild-type and mutant $hA_{2A}AR$ (Figure 2). Wild-type and mutant receptors were expressed efficiently at similar levels.

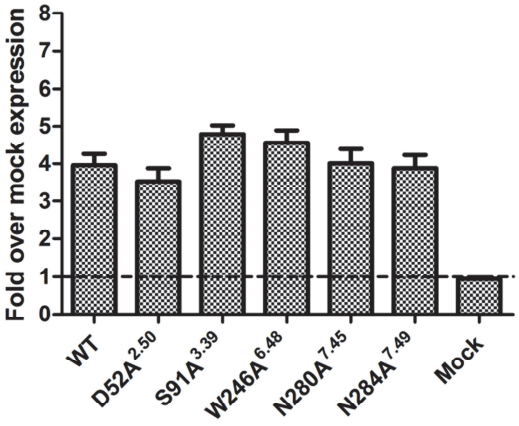

Figure 2. Receptor expression levels on the cell surface of HEK293 cells transiently transfected with wild-type $hA_{2A}AR$ or $D52A^{2.50}$, $S91A^{3.39}$, $W246A^{6.48}$, $N280A^{7.45}$, or $N284A^{7.49}$ single point mutated $hA_{2A}AR$, represented as fold-over-mock transfected HEK293T cells. The figure represents data combined from at least two separate experiments performed in quadruplicate.

Homologous competition assays

First we analyzed the effect of mutation of these residues on the affinity of radioligands [^{3}H]NECA (agonist) and [^{3}H]ZM-241,385 (antagonist) in the absence of NaCl (Table 1). The affinity of [^{3}H]NECA and [^{3}H]ZM-241,385 for the wild-type $hA_{2A}AR$ was 81 nM and 4.6 nM, respectively. $D52A^{2.50}$ showed the same affinity as the wild-type receptor for both radioligands (77 nM and 3.5 nM, respectively). The other mutations caused some decrease in affinity for both radioligands, with a more pronounced effect on the agonist. An approximately 3-fold decrease of [^{3}H]NECA affinity was observed for receptors with mutations $S91A^{3.39}$ and $N284A^{7.49}$, while [^{3}H]ZM-241,385's affinity did not change significantly by these mutations. Radioligand agonist affinity decreased approximately 9-fold on $N280A^{7.45}$, while a 1.8-fold decrease was observed for the antagonist. The $W246A^{6.48}$ mutation affected affinities most, i.e. a 24-fold decrease in [^{3}H]NECA affinity and a 5-fold decrease in [^{3}H]ZM-241,385 affinity.

Table 1. Homologous competition displacement studies yielding K_D values (nM) for [^{3}H]NECA and [^{3}H]ZM-241,385 binding to wild-type human A_{2A}AR and single point mutants D52A$^{2.50}$, S91A$^{3.39}$, W246A$^{6.48}$, N280A$^{7.45}$, and N284A$^{7.49}$, transiently expressed on HEK293 cell membranes.

	[^{3}H]NECA		[^{3}H]ZM-241,385	
	K_D (nM)	Change[a]	K_D (nM)	Change[a]
Wild-type	81 ± 5	1.0	4.6 ± 0.5	1.0
D52A$^{2.50}$	77 ± 8	1.0	3.5 ± 0.5	0.75
S91A$^{3.39}$	258 ± 24***	3.2	7.0 ± 0.2	1.5
W246A$^{6.48}$	1942 ± 124***	24	23.2 ± 4.3***	5.0
N280A$^{7.45}$	752 ± 147***	9.3	8.4 ± 1.3*	1.8
N284A$^{7.49}$	237 ± 27***	2.9	7.0 ± 0.7	1.5

a: Change in fold over wild-type.
Significantly different from wild-type with * $p < 0.05$ or *** $p < 0.001$ (one-way ANOVA with Dunnett's post test performed on corresponding pK_D values).
Values are means ± SEM of at least three separate assays performed in duplicate.

Concentration-effect curves in radioligand displacement studies

Displacement curves of [^{3}H]ZM-241,385 and [^{3}H]NECA binding were recorded with different concentrations of NaCl, amiloride, and its more lipophilic derivative HMA for the wild-type and mutant receptors (Figure 3). Whenever possible, IC_{50} values were derived for the inhibitory modulation of agonist [^{3}H]NECA and antagonist [^{3}H]ZM-241,385 binding by NaCl, amiloride, and HMA (Tables 2 and 3). NaCl inhibited [^{3}H]NECA binding to the wild-type receptor with an IC_{50} value of 44 ± 6 mM. At the highest concentration tested (1 M) NaCl had modest effects with 59 ± 3 %, 89 ± 2 %, and 52 ± 11 % of [^{3}H]NECA binding remaining on mutants S91A$^{3.39}$, N280$^{7.45}$, and W246A$^{6.48}$, respectively (Figure 3A). [^{3}H]NECA binding was not inhibited by NaCl on mutant N284A$^{7.49}$ (Figure 3A). Increasing concentrations of NaCl showed a tendency to enhance [^{3}H]ZM-241,385 binding to the wild-type receptor as well as to the mutants tested, with W246A$^{6.48}$ showing the biggest enhancement (Figure 3B). At the highest concentration of NaCl (1 M), [^{3}H]NECA agonist binding was also enhanced in the mutant receptor D52A$^{2.50}$ (172 ± 9 %), which suggests that at such extreme concentrations NaCl can exert allosteric effects that are different from the specific effect of sodium ion binding at Asp52$^{2.50}$.

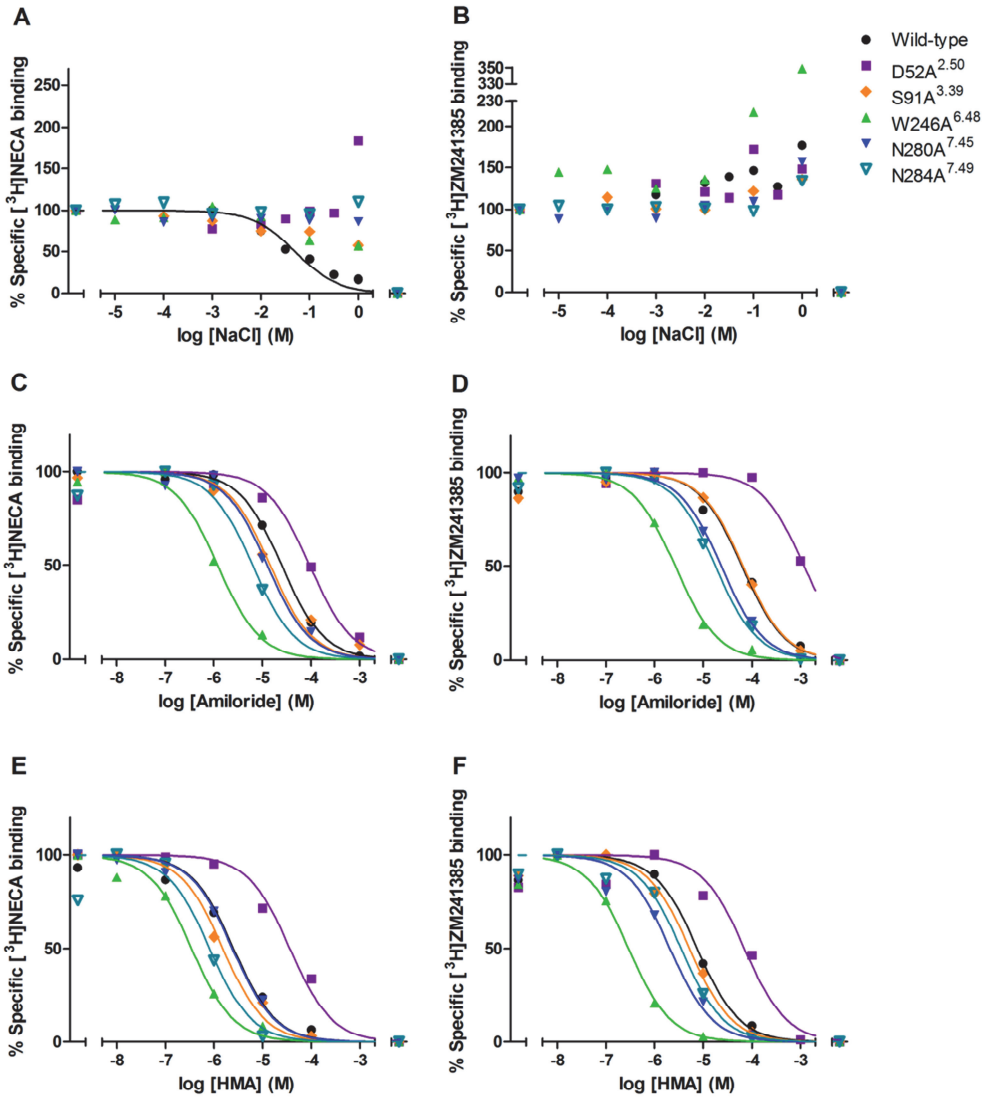

Figure 3. Displacement/enhancement of specific [^{3}H]NECA **(A, C, E)** and [^{3}H]ZM-241,385 **(B, D, F)** binding by NaCl **(A, B)**, amiloride **(C, D)**, and HMA **(E, F)** on wild-type human A_{2A}AR and point mutants D52A$^{2.50}$, S91A$^{3.39}$, W246A$^{6.48}$, N280A$^{7.45}$, and N284A$^{7.49}$ transiently expressed on HEK293T cell membranes. Representative graphs from one experiment performed in duplicate are shown.

Table 2. Displacement of specific [^{3}H]NECA binding by amiloride and HMA from wild-type human A_{2A}AR and point mutants D52A$^{2.50}$, S91A$^{3.39}$, W246A$^{6.48}$, N280A$^{7.45}$, N284A$^{7.49}$ transiently expressed on HEK293 cell membranes.

	[^{3}H]NECA			
	Amiloride		HMA	
	IC_{50} (μM)	Change[a]	IC_{50} (μM)	Change[a]
Wild-type	16 ± 3	1.0	2.5 ± 0.4	1.0
D52A$^{2.50}$	175 ± 75***	11	35 ± 9***	14
S91A$^{3.39}$	13 ± 1.8	0.81	2.3 ± 0.6	0.92
W246A$^{6.48}$	2.7 ± 0.9***	0.17	0.43 ± 0.05***	0.17
N280A$^{7.45}$	10 ± 2	0.63	2.4 ± 0.6	1.0
N284A$^{7.49}$	5.9 ± 1.4	0.37	1.0 ± 0.3*	0.40

a: Change in fold over wild-type.
Significantly different from wild-type with * $p < 0.05$ or *** $p < 0.001$ (one-way ANOVA with Dunnett's post test performed on corresponding pIC_{50} values).
Values are means ± SEM of at least three separate assays performed in duplicate.

Amiloride and HMA were capable of displacing [^{3}H]NECA and [^{3}H]ZM-241,385 binding on the point mutant receptors (Figures 3C-F), although with different IC_{50} values with respect to the wild-type receptor (Tables 2 and 3). D52A$^{2.50}$ was particularly insensitive to amilorides: the inhibitory potency of amiloride and HMA on [^{3}H]NECA binding was decreased by 11- and 14-fold and on [^{3}H]ZM-241,385 binding by 17- and 18-fold, respectively. Conversely, W246A$^{6.48}$ showed an increased inhibitory potency of amiloride and HMA, both on [^{3}H]NECA (6-fold for both amilorides) and on [^{3}H]ZM-241,385 (24- and 25-fold, respectively) binding. For N280A$^{7.45}$ we observed a smaller but also significant increase (3.6-fold) of the negative modulation of [^{3}H]ZM-241,385 binding by HMA, and for N284A$^{7.49}$ a similar increase (2.6-fold) of the modulation of both [^{3}H]NECA and [^{3}H]ZM-241,385 binding by HMA. For N284A$^{7.49}$ the potency of amiloride increased significantly only in case of [^{3}H]ZM-241,385 displacement. Mutant S91A$^{3.39}$ exhibited similar potencies as the wild-type receptor for displacement of both radioligands by amiloride and HMA (Tables 2 and 3). These observations suggest that while polar interactions with W246A$^{6.48}$, N280A$^{7.45}$ and N284A$^{7.49}$ are important for binding of the sodium ion and coordinating water molecules, the interactions of amilorides with these three side chains are somewhat suboptimal.

Table 3. Displacement of specific [^{3}H]ZM-241,385 binding by amiloride and HMA from wild-type human A_{2A}AR and point mutants D52A$^{2.50}$, S91A$^{3.39}$, W246A$^{6.48}$, N280A$^{7.45}$, N284A$^{7.49}$ transiently expressed on HEK293 cell membranes.

	[^{3}H]ZM-241,385			
	Amiloride		HMA	
	IC_{50} (μM)	Change[a]	IC_{50} (μM)	Change[a]
Wild-type	63 ± 16	1.0	8.9 ± 1.5	1.0
D52A$^{2.50}$	1065 ± 274***	17	164 ± 47***	18
S91A$^{3.39}$	82 ± 8	1.3	8.2 ± 0.5	0.92
W246A$^{6.48}$	2.6 ± 0.4***	0.04	0.36 ± 0.06***	0.04
N280A$^{7.45}$	20 ± 4	0.32	2.5 ± 0.6**	0.28
N284A$^{7.49}$	16 ± 4*	0.25	3.3 ± 0.8*	0.37

a: Change in fold over wild-type.
Significantly different from wild-type with * $p < 0.05$, ** $p < 0.01$, or *** $p < 0.001$ (one-way ANOVA with Dunnett's post test performed on corresponding pIC_{50} values).
Values are means ± SEM of at least three separate assays performed in duplicate.

Concentration-effect curves for cAMP production

Functional assays were performed to further characterize the effect of the single point mutations on hA_{2A}AR signaling. As an agonist CGS-21680 was used to activate the receptor, yielding an increase in cAMP production through G_s protein activation (Figure 4 and Table 4). The use of the selective agonist CGS-21680 for the hA_{2A}AR rather than the nonselective NECA ensured that no endogenously expressed hA_{2B}AR was activated in the HEK293 cells. The absence of activation by 10 μM CGS-21680 in the untransfected parental cell line confirmed that indeed no endogenously expressed receptor was activated in this experimental setup. Mutations of the residues involved in the sodium ion binding site affected basal activity and efficacy of cAMP signaling by the hA_{2A}AR. D52A$^{2.50}$ and N284A$^{7.49}$ mutants showed neither basal activity nor any activation by CGS-21680. In all other cases, the mutant receptor showed a dramatically decreased receptor signaling response to CGS-21680 binding (E_{max}-E_{basal}), ranging from only 27 % to 46 % of the wild-type response. The basal activity significantly increased over wild-type in mutation S91A$^{3.39}$. The N280A$^{7.45}$ mutant also showed a tendency to increased basal activity but this was not significantly different from wild-type. This constitutive activity was inhibited by addition of 10 μM ZM-241,385, confirming that the elevated basal cAMP production in the transiently transfected cells was caused by these mutant receptors (supplemental Figure

S1). CGS-21680 activated both the wild-type and mutant N280A$^{7.45}$ hA_{2A}AR with an EC_{50} value of 17 nM. The potency of CGS-21680 was somewhat decreased on mutant W246A$^{6.48}$ (~5-fold). In the case of S91A$^{3.39}$ the difference between basal and maximum activity was judged too small to derive an accurate EC_{50} value.

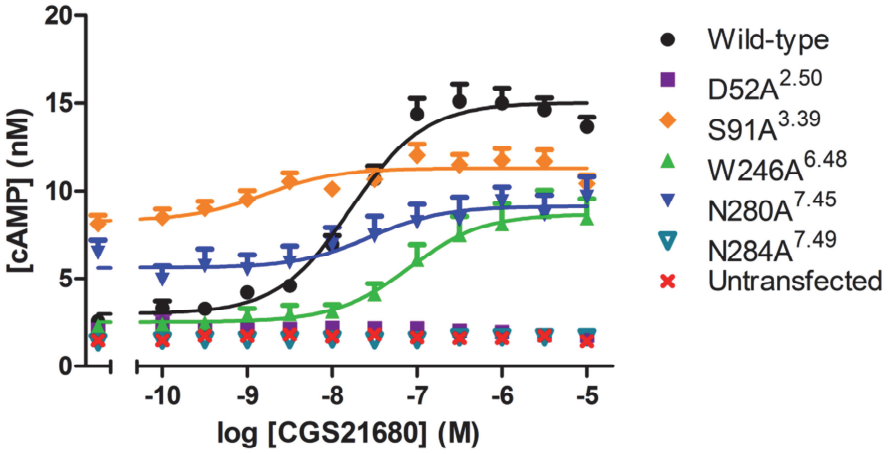

Figure 4. Full concentration-effect curves of hA_{2A}AR selective agonist CGS-21680 induced stimulation of cAMP production by HEK293T cells stably expressing wild-type, transiently expressing D52A$^{2.50}$, S91A$^{3.39}$, W246A$^{6.48}$, N280A$^{7.45}$, or N284A$^{7.49}$ hA_{2A}AR, or by untransfected parental HEK293T cells. Graphs represent mean ± SEM from at least three separate experiments performed in triplicate.

Molecular dynamics simulations

The dynamic behaviors of the wild-type receptor and the receptors with mutated residues important for sodium ion coordination D52A$^{2.50}$, S91A$^{3.39}$, W246A$^{6.48}$, N280A$^{7.45}$, and N284A$^{7.49}$, were simulated with either only antagonist ZM-241,385 present or with both ZM-241,385 in the orthosteric pocket and the sodium ion in its allosteric binding site (Supplemental Table S1). In addition, the wild-type receptor and mutated receptors D52A$^{2.50}$ and W246A$^{6.48}$ were simulated with ZM-241,385 in the orthosteric pocket and amiloride or HMA in the sodium ion binding site. Analysis of the root mean squared deviation (RMSD) revealed equilibrated trajectories typically after 20-30 ns with an average value of 1.8 Å in all simulations, and analysis of the root mean squared fluctuation (RMSF) confirmed no major conformational changes in the receptor due to any of the mutations.

Table 4. Agonist activation of wild-type and mutant adenosine A_{2A} receptor. cAMP production by HEK293T cells stably expressing wild-type or transiently transfected with D52A$^{2.50}$, S91A$^{3.39}$, W246A$^{6.48}$, N280A$^{7.45}$, or N284A$^{7.49}$ $hA_{2A}AR$, was measured in presence of increasing concentrations of CGS-21680.

	CGS-21680		
	pEC_{50} (EC_{50}[a])	**Change[b]**	**% Response[c]**
Wild-type	7.8 ± 0.0 (17)	1.0	100 ± 14
D52A$^{2.50}$	N.D.[d]	N.D.[d]	-2 ± 1***
S91A$^{3.39}$	N.D.[e]	N.D.[e]	27 ± 11***
W246A$^{6.48}$	7.1 ± 0.0*** (86)	5.1	46 ± 13**
N280A$^{7.45}$	7.8 ± 0.1 (17)	1.0	29 ± 12***
N284A$^{7.49}$	N.D.[d]	N.D.[d]	2 ± 2***

a: EC_{50} (nM) in parentheses.
b: Change in fold over wild-type.
c: % Signaling response of receptor to CGS-21680 (E_{max} - E_{basal}) in % of wild-type response.
d: No stimulation of cAMP was observed with 10 µM CGS-21680.
e: Basal activity was too high to determine an accurate EC_{50} value.
Significantly different from wild-type with ** $p < 0.01$ or *** $p < 0.001$ (one-way ANOVA with Dunnett's post test).
pEC_{50} and % response values are means ± SEM of at least three separate assays performed in triplicate.

The effect of each single point mutation on the sodium ion mobility and coordination was assessed (Table 5). During the simulation in the wild-type model conducted in Chapter 3 the sodium ion alternated between two resonance positions, in which the sodium ion had a direct interaction with either Ser91$^{3.39}$ (22% occurrence of direct interaction during the simulations) or Asn280$^{7.45}$ (29%), while maintaining a continuous direct interaction with Asp52$^{2.50}$ (90%). In mutation D52A$^{2.50}$ however, sodium ion mobility increased by 5-fold and almost no direct interactions with residues Ser91$^{3.39}$ (1%) and Asn280$^{7.49}$ (0%) occurred. In the first 10 ns of the simulation with the D52A$^{2.50}$ mutant receptor, the sodium ion migrated from its starting position in the sodium ion binding site near Ala52$^{2.50}$ to a vestibular pocket formed by residues Glu13$^{1.39}$ and His278$^{7.43}$, where the sodium ion remained stable for the remaining 90 ns of the simulation (Figure 5). In contrast, mutants S91A$^{3.39}$, W246A$^{6.48}$, N280A$^{7.45}$ or N284A$^{7.49}$ did not show major deviations as compared to the wild-type situation with regards to either the ion mobility or the average number of oxygen atoms coordinating it (Supplemental Table S2),[23] due to the replacement of the mutated side chain by an additional water molecule. However, the occurrence of direct

interactions with the three coordinating residues appeared lowered to some extent, indicative of a non-optimal ion coordination by these mutants. This was true in particular for the interaction with Asp52$^{2.50}$ (51-76%, see Table 5).

Mobility and interactions with the receptor of amiloride and HMA, as docked in the sodium ion binding site, were assessed in simulations of the wild-type receptor and mutant receptors D52A$^{2.50}$ and W246A$^{6.48}$ (Figure 6). In these relatively short MD runs amiloride was equally stable in the proposed binding site upon both mutations, with an RMSF value of approx. 2 Å. The mobility of the amiloride derivative HMA was increased 3-fold by mutation D52A$^{2.50}$, and in one out of three simulations it left the putative binding pocket following the same pathway as depicted in Figure 5B. Mutation W246A$^{6.48}$, on the contrary, did not affect HMA stability in the same way. However, it is worth noting that specific contacts changed for the two ligands with both mutants. In the wild-type receptor, both ligands achieved an average number of 4 simultaneous hydrogen bonds, mainly with residues Asp52$^{2.50}$ and Trp246$^{6.48}$ (Supplemental Figure S2 and Chapter 3). For amiloride, the number of hydrogen bonds dropped to approx. 2 in the two mutants examined, as well as for HMA with mutant W246A$^{6.48}$, while mutation D52A$^{2.50}$ had a more dramatic effect on HMA with only one hydrogen bond left on average (Supplemental Figure S2). Note that in this analysis, interactions between amino (amilorides) and carbonyl (Asp52$^{2.50}$) groups were approximated as hydrogen bonds, instead of the stronger salt bridge interactions that occur in reality, the loss of which is expected to have a large effect on the affinities of amilorides. This analysis did not reveal stable hydrogen bonds of amilorides with either of the asparagines close by (Asn280$^{7.45}$ and Asn284$^{7.49}$).

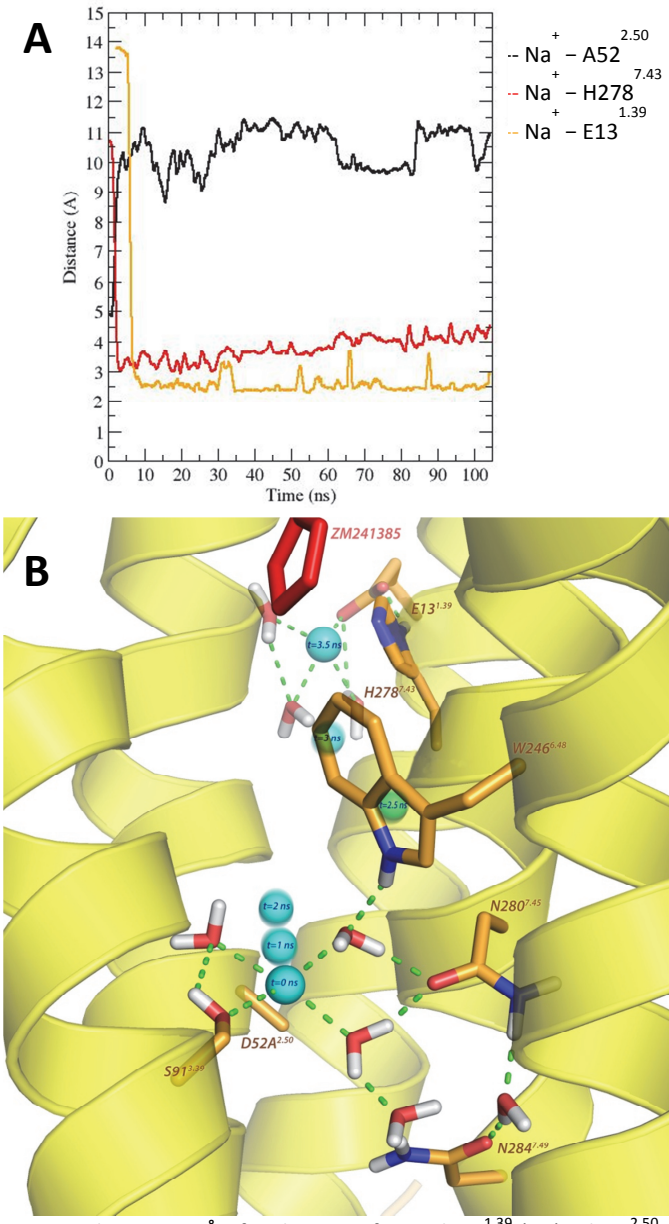

Figure 5. A) Average distance in Å of sodium ion from Glu13$^{1.39}$ (Oε), Ala52$^{2.50}$ (Cα), and His278$^{7.43}$ (Nδ) as a function of the simulation time for the D52A$^{2.50}$ mutant. Graphs represent means from three independent simulations. **B)** 3D representation of the migration pathway of the sodium ion (cyan sphere, with labels indicating the occupancy at averaged MD simulation windows) from its putative binding site towards the vestibular pocket formed by Glu13$^{1.39}$ and His278$^{7.43}$. The residues and water molecules interacting with the sodium ion are represented in sticks, and hydrogen bonds represented by green dotted lines.

Table 5. Mobility of the sodium ion in root mean squared fluctuation (RMSF) in wild-type and mutant receptor, and the occurrence in % of direct interactions with the different residues coordinating the ion in the crystal structure along the simulation time.

	Na^+ mobility *RMSF in Å*	Na^+ interactions *% occurrence with indicated residues*		
		Asp52$^{2.50}$	**Ser91$^{3.39}$**	**Asn280$^{7.45}$**
Wild-type	2.5 ± 0.3	89.6 ± 7.8	22.3 ± 10.3	28.7 ± 5.4
D52A$^{2.50}$	11.2 ± 0.3*	-	1.1 ± 0.2*	0.0 ± 0.0*
S91A$^{3.39}$	1.8 ± 0.2	75.6 ± 5.9	-	25.5 ± 2.9
W246A$^{6.48}$	2.5 ± 0.3	51.1 ± 7.9*	17.1 ± 6.2	10.0 ± 4.3*
N280A$^{7.45}$	2.6 ± 0.2	67.1 ± 0.7*	12.4 ± 3.1	-
N284A$^{7.49}$	2.6 ± 0.1	75.5 ± 7.3	3.8 ± 1.5*	25.6 ± 17.9

RMSF values are means ± SEM of three separate 100 ns simulations.
% interaction occurrence values are means ± SEM of three separate 100 ns simulations.
Significantly different from control with * $p < 0.05$ (Student's t-test).

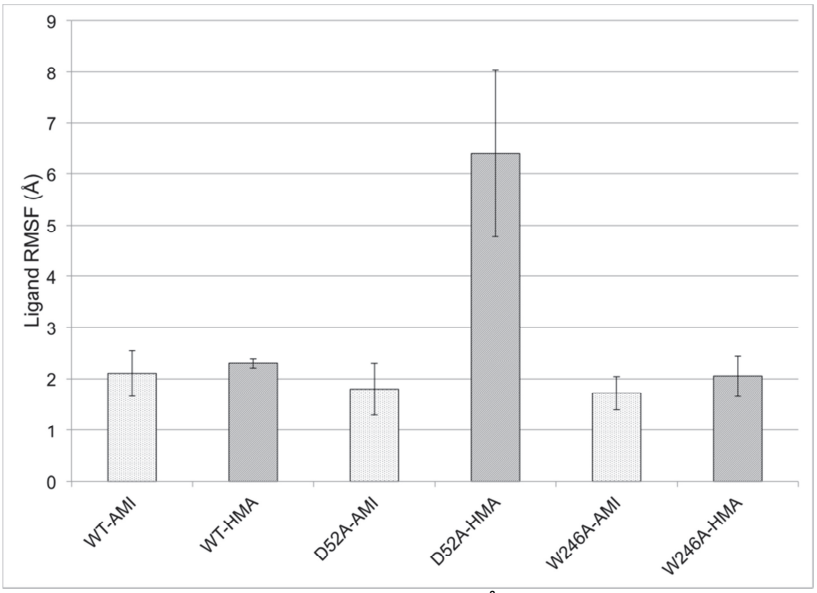

Figure 6. Root mean squared fluctuation (RMSF, Y axis, in Ångstrom) of amiloride (AMI, dotted bars) or HMA (gray bars) indicating their mobility in the wild-type (WT) or mutant forms D52A$^{2.50}$ and W246A$^{6.48}$. The figures represent data (± SD) combined from three independent simulations of 100 ns.

Discussion

The sodium ion binding site appears conserved amongst class A GPCRs.[24] Subsequent to the $hA_{2A}AR$ the crystal structures of the human protease-activated receptor 1,[25] the β_1-adrenergic receptor,[26, 27] and the human δ-opioid receptor[28] further confirmed the common role of this site in the inactive conformation of GPCRs. A sequence comparison of the sodium ion binding site between more distant class A GPCRs shows that individual amino acids may differ, but collectively they apparently maintain the properties to coordinate a sodium ion.

These observations made us examine the residues involved in the $hA_{2A}AR$ sodium ion binding site in more detail, through a combined approach of mutational and computational studies. Most importantly, we learned that all mutations in the sodium ion binding pocket impact A_{2A} receptor signaling significantly, including both constitutive and agonist-stimulated activity. Although all mutant data in the present study is novel, we have shown a number of similar findings on the wild-type receptor before (Chapter 3 and Lane et al.),[29] indicative of the robustness of the assay system. We will discuss our findings in the light of available mutation data in literature, by examining the mutated amino acids individually. For the search we made use of data available in the GPCRDB.[30]

$Asp^{2.50}$. The pronounced effects of mutation of the conserved $Asp^{2.50}$ are in agreement with previous studies. Mutation of $Asp^{2.50}$ abolished the effect of NaCl on agonist binding in studies on a multitude of GPCRs, for example in the α_2-adrenergic receptor,[31] dopamine D_2,[32] adenosine A_1,[33] adenosine A_3,[34] and δ-opioid receptors.[28] In MD simulations of the wild-type $hA_{2A}AR$ $Asp52^{2.50}$ dominated coordination of the sodium ion (Chapter 3). Mutation of $Asp^{2.50}$ is known to silence signaling in many GPCRs.[5] The migration of the sodium ion to $Glu13^{1.39}$ and $His278^{7.43}$ agrees with the involvement of these amino acids in sodium ion allosterism observed previously by Gao et al.[35] From a reversed perspective, this simulation could envisage a pathway for the entrance of the sodium ion, which should occur from the extracellular side according to the physiological gradient,[6, 36] and where residue $Glu13^{1.39}$, conserved in all adenosine receptors, could stabilize such a pathway. The enhancement of agonist binding to the $D52A^{2.50}$ mutant at high (1 M) concentrations of NaCl suggests that binding of the ion to alternative sites may produce further allosteric effects, different from the effects on wild-type $Asp52^{2.50}$.

The affinities of amiloride and HMA were 10 – 20-fold decreased on the Asp52$^{2.50}$ mutant receptor (Tables 2 and 3), strongly suggesting that the positively charged guanidinium moiety of the compounds interacts with the negatively charged aspartic acid. A more modest, 4-fold, decrease in affinity for an amiloride derivative has been reported for the D_4 dopamine receptor by mutation D$^{2.50}$N.[37] In adenosine A_3 and α_2-adrenergic receptors affinities of amiloride and its derivatives were largely undisturbed by mutation D$^{2.50}$N,[31, 34] suggesting that the more drastic mutation to Ala in the current study more precisely revealed the importance of this residue for amiloride binding.

Trp$^{6.48}$. It appeared that sodium ions and agonist NECA can bind simultaneously to the W246A$^{6.48}$ receptor (Figure 3A), in contrast with the *wild-type* receptor where NECA and sodium ion binding are mutually exclusive (Chapter 3). Conversely, mutant W246A$^{6.48}$ augmented the positive effect of sodium ions on antagonist ZM-241,385 binding (Figure 3B). It seems that Trp246$^{6.48}$ may clash with both agonists and antagonists in the orthosteric pocket, as the absence of this residue has a positive effect on binding of both agonists and antagonists in presence of the sodium ion. Trp$^{6.48}$, conserved in many GPCRs, has long been suggested to act as a "toggle switch" in receptor activation,[38] but has never been studied in the context of allosteric modulation by sodium ions. It has been mutated to both Phe and Ala in the human adenosine A_3 receptor, being the closest homolog to the A_{2A} receptor.[34, 39] Interestingly, agonist binding was hardly affected by these mutations, whereas antagonists showed a modest decrease in affinity. Receptor activation, however, was largely impeded, seemingly more than our current findings on the A_{2A} receptor (see e.g. Figure 4).

Remarkably, the affinities for amiloride and HMA were strongly increased on this mutant (Tables 2 and 3), suggesting that the wild-type tryptophan creates a substantial steric strain for the binding of amilorides. In the adenosine A_3 receptor the W$^{6.48}$A mutation increased HMA potency on agonist binding as well.[34] The mobility of amiloride and HMA was unaffected by the W246A$^{6.48}$ mutation (Figure 6), which indicates that the weakened polar interactions (Supplemental Figure S2) are compensated by the absence of steric strain with Trp246$^{6.48}$ in this mutant. The collision of the bulkier azepane group of HMA with Trp246$^{6.48}$ in the wild-type receptor may result in a loosened interaction with the receptor, which explains HMA's increased mobility by mutation D52A$^{2.50}$ compared to

amiloride. In Chapter 3, the more substantial steric clash of HMA with Trp246$^{6.48}$ compared to amiloride had been observed as well.

Ser$^{3.39}$, Asn$^{7.45}$, and Asn$^{7.49}$. In the wild-type receptor the sodium ion alternates direct interactions with Ser91$^{3.39}$ and Asn280$^{7.45}$ in two distinct resonance positions, as predicted in MD simulations (Table 5 and Chapter 3), while maintaining contact with Asp52$^{2.50}$. This is in agreement with the observation that sodium ion modulation of agonist binding is not completely abolished in mutant receptors S91A$^{3.39}$ and N280A$^{7.45}$ (Figure 3A), and that the two remaining residues in mutants S91A$^{3.39}$ and N280A$^{7.45}$ (Asp52$^{2.50}$, and Asn280$^{7.45}$ or Ser91$^{3.39}$, respectively) still interact directly with the sodium ion, although less than in the wild-type receptor (Table 5). Jiang et al. had found that the same S91A mutation did not affect orthosteric ligand binding very much,[40] even less so than the slight decrease in affinity in our experiments (Table 1). In the adenosine A_1 receptor however, orthosteric ligand binding could not be detected for this mutation, maybe due to lack of expression.[33]

In mutant N284A$^{7.49}$ sodium ion modulation of agonist binding was completely abolished (Figure 3A). In the antagonist-bound inactive conformation of the receptor, Asn284$^{7.49}$ might improve sodium ion coordination through stabilization of the side chain of Asp52$^{2.50}$, explaining the disruption of sodium ion binding by mutation N284A$^{7.49}$. The same role of Asn$^{7.49}$ in stabilization of Asp$^{2.50}$ was proposed previously in e.g., the histamine H_1 and thyrotropin receptors.[41, 42] At the same time, in the agonist-bound structure of the A_{2A}AR residues Asn280$^{7.45}$ and Asn284$^{7.49}$ form a hydrogen bond, possibly stabilizing the collapsed state of the pocket that excludes sodium ion binding.[8, 43] Consequently, mutations N280A$^{7.45}$ and N284A$^{7.49}$ might facilitate the formation of the uncollapsed state of the sodium ion pocket and shift the receptor away from the active state, even when the sodium ion is not present in its binding site. Our results support this hypothesis, as mutation of either residue decreases agonist affinity drastically, while antagonist affinity is only slightly decreased (Table 1), sodium ions inhibit agonist binding only weakly (N280A$^{7.45}$) or not at all (N284A$^{7.49}$, Figure 3A). In the adenosine A_1 receptor mutation N$^{7.49}$C increased antagonist binding slightly, which could point to a similar mechanism.[44] Moreover, mutation N284A$^{7.49}$ abolished agonist activation completely (Table 4). Correspondingly, Asn284$^{7.49}$ is part of the highly conserved NP*XX*Y motif, involved in GPCR activation.[38, 45]

Mutants N280A$^{7.45}$ and N284A$^{7.49}$ generally affected the potencies of amilorides in a positive way, in particular for HMA Figures 3E, F and Tables 2, 3). According to the binding mode proposed in Chapter 3, the nitrogen atoms in the amide moiety of both asparagines lie close to the guanidinium group of both amilorides coordinated by Asp52$^{2.50}$, yet they only make sporadic H-bond contacts (Supplemental Figure S2). Thus alanine substitutions might indeed facilitate binding of amilorides by avoiding unfavorable polar interactions (Asn280$^{7.45}$) or by allowing more conformational freedom to Asp52$^{2.50}$ (Asn284$^{7.49}$), accommodating in particular the bulky HMA and enhancing its binding.

The MD simulations showed only minor effects on the capacity of mutants S91A$^{3.39}$, W246A$^{6.48}$, N280A$^{7.45}$, and N284A$^{7.49}$ to bind the sodium ion in the inactive conformation of the receptor. This seems in contrast to the greatly reduced sensitivity of these mutants to physiological concentrations of NaCl (Figure 3A). In addition to the explanations discussed above, an alternative explanation arises from the observation that each of these four side chain annihilations creates additional room for an extra water molecule, thus fulfilling the coordination number of the ion (Supplemental Table S2). This might allow that, in contrast to the wild-type receptor, the mutants also bind the sodium ion in an active receptor conformation, resulting in the observed loss of modulatory effect on agonist binding.

In conclusion, our results show the importance of the sodium ion binding site in orthosteric ligand binding and receptor activity. Mutation D52A$^{2.50}$ caused an immediate displacement of the sodium ion to a distant pocket in MD simulations, in agreement with the loss of the modulatory effect in our molecular pharmacology experiments. The effects of the other mutations were varied, but they significantly affected sodium ion modulation of agonist binding and modulation by amilorides of both agonist and antagonist binding. In addition, all mutations influenced receptor activation, particularly by affecting the levels of constitutive and agonist-stimulated activity, emphasizing the importance of the sodium ion binding pocket for the receptor's active conformation(s). These findings imply that because of allosterism by sodium ions and amilorides, the sodium ion binding pocket is a prominent player in receptor functionality and ligand affinity. Our study also opens the door to the design of novel synthetic allosteric modulators or bitopic ligands connecting the sodium ion binding site and the orthosteric binding pocket.

Supplemental information

Supplemental information includes Figures S1 and S2, and Tables S1 and S2, and can be found with this article online at dx.doi.org/10.1124/mol.114.095737

Acknowledgments

This work was supported by the Netherlands Organization for Scientific Research - Chemical Sciences (Grant 714.011.001), the Swedish Research Council (Grant 521-2014-2118*),* the Swedish strategic research program eSSENCE, and the Swedish National Infrastructure for Computing.

References

1. Rask-Andersen M, Almén MS, and Schiöth HB, *Trends in the exploitation of novel drug targets.* Nat Rev Drug Discovery, 2011. 10(8): p. 579-90.
2. Katritch V, Cherezov V, and Stevens RC, *Structure-function of the G protein-coupled receptor superfamily.* Annu Rev Pharmacol Toxicol, 2013. 53: p. 531-56.
3. Chen JF, Eltzschig HK, and Fredholm BB, *Adenosine receptors as drug targets — what are the challenges?* Nat Rev Drug Discovery, 2013. 12(4): p. 265-86.
4. Liu W, Chun E, Thompson AA, et al., *Structural basis for allosteric regulation of GPCRs by sodium ions.* Science, 2012. 337(6091): p. 232-36.
5. Parker MS, Wong YY, and Parker SL, *An ion-responsive motif in the second transmembrane segment of rhodopsin-like receptors.* Amino Acids, 2008. 35(1): p. 1-15.
6. Selent J, Sanz F, Pastor M, et al., *Induced effects of sodium ions on dopaminergic G-protein coupled receptors.* PLoS Comput Biol, 2010. 6(8): p. e1000884.
7. Ballesteros JA and Weinstein H, *Integrated methods for the construction of three-dimensional models and computational probing of structure-function relations in G protein-coupled receptors*, in *Methods Neurosci*. 1995, Academic Press: San Diego. p. 366-428.
8. Xu F, Wu H, Katritch V, et al., *Structure of an agonist-bound human A_{2A} adenosine receptor.* Science, 2011. 332(6027): p. 322-7.
9. Sambrook J, Fritsch EF, and Maniatis T, *Molecular Cloning: A Laboratory Manual*. 2nd ed. 1989, New York: Cold Spring Harbor Laboratory Press.
10. Smith PK, Krohn RI, Hermanson GT, et al., *Measurement of protein using bicinchoninic acid.* Anal Biochem, 1985. 150(1): p. 76-85.
11. Schrödinger LLC, *Maestro, version 9.3*. 2012: New York.
12. Hess B, Kutzner C, van der Spoel D, et al., *GROMACS 4: algorithms for highly efficient, load-balanced, and scalable molecular simulation.* J Chem Theory Comput, 2008. 4(3): p. 435-47.
13. Rodríguez D, Piñeiro A, and Gutiérrez-de-Terán H, *Molecular dynamics simulations reveal insights into key structural elements of adenosine receptors.* Biochemistry, 2011. 50(19): p. 4194-208.
14. Gutiérrez-de-Terán H, Bello X, and Rodriguez D, *Characterization of the dynamic events of GPCRs by automated computational simulations.* Biochem Soc Trans, 2013. 41(1): p. 205-12.

15. Kaminski GA, Friesner RA, Tirado-Rives J, et al., *Evaluation and reparametrization of the OPLS-AA force field for proteins via comparison with accurate quantum chemical calculations on peptides.* J Phys Chem B, 2001. 105(28): p. 6474-87.
16. Schrödinger LLC, *Macromodel, version 9.7*. 2009: New York.
17. Berger O, Edholm O, and Jähnig F, *Molecular dynamics simulations of a fluid bilayer of dipalmitoylphosphatidylcholine at full hydration, constant pressure, and constant temperature.* Biophys J, 1997. 72(5): p. 2002-13.
18. Chakrabarti N, Neale C, Payandeh J, et al., *An iris-like mechanism of pore dilation in the CorA magnesium transport system.* Biophys J, 2010. 98(5): p. 784-92.
19. Berendsen HJC, Postma JPM, Van Gunsteren WF, et al., *Interaction models for water in relation to protein hydration*, in *Intermolecular Forces*, B. Pullman, Editor. 1981, D. Reidel Publishing Company: Dordrecht. p. 331-42.
20. Nose S and Klein ML, *Constant pressure molecular dynamics for molecular systems.* Mol Phys, 1983. 50(5): p. 1055-76.
21. Humphrey W, Dalke A, and Schulten K, *VMD - visual molecular dynamics.* J Mol Graph, 1996. 14(1): p. 33-8.
22. Schrödinger LLC, *The PyMOL Molecular Graphics System, version 1.5.0.4*. New York.
23. Harding MM, *Small revisions to predicted distances around metal sites in proteins.* Acta Crystallogr D Biol Crystallogr, 2006. 62(Pt 6): p. 678-82.
24. Katritch V, Fenalti G, Abola EE, et al., *Allosteric sodium in class A GPCR signaling.* Trends Biochem Sci, 2014. 39(5): p. 233-44.
25. Zhang C, Srinivasan Y, Arlow DH, et al., *High-resolution crystal structure of human protease-activated receptor 1.* Nature, 2012. 492(7429): p. 387-92.
26. Christopher JA, Brown J, Doré AS, et al., *Biophysical fragment screening of the β_1-adrenergic receptor: identification of high affinity arylpiperazine leads using structure-based drug design.* J Med Chem, 2013. 56(9): p. 3446-55.
27. Miller-Gallacher JL, Nehmé R, Warne T, et al., *The 2.1 Å resolution structure of cyanopindolol-bound β_1-adrenoceptor identifies an intramembrane Na^+ ion that stabilises the ligand-free receptor.* PLoS ONE, 2014. 9(3): p. e92727.
28. Fenalti G, Giguere PM, Katritch V, et al., *Molecular control of δ-opioid receptor signalling.* Nature, 2014. 506(7487): p. 191-6.
29. Lane JR, Klein Herenbrink C, Van Westen GJP, et al., *A novel nonribose agonist, LUF5834, engages residues that are distinct from those of adenosine-like ligands to activate the adenosine A_{2A} receptor.* Mol Pharmacol, 2012. 81(3): p. 475-87.
30. Isberg V, Vroling B, Van der Kant R, et al., *GPCRDB: an information system for G protein-coupled receptors.* Nucleic Acids Res, 2014. 42(Database issue): p. D422-5.
31. Horstman DA, Brandon S, Wilson AL, et al., *An aspartate conserved among G-protein receptors confers allosteric regulation of α_2-adrenergic receptors by sodium.* J Biol Chem, 1990. 265(35): p. 21590-5.
32. Neve KA, Cox BA, Henningsen RA, et al., *Pivotal role for aspartate-80 in the regulation of dopamine D_2 receptor affinity for drugs and inhibition of adenylyl cyclase.* Mol Pharmacol, 1991. 39(6): p. 733-9.
33. Barbhaiya H, McClain R, IJzerman AP, et al., *Site-directed mutagenesis of the human A_1 adenosine receptor: influences of acidic and hydroxy residues in the first four transmembrane domains on ligand binding.* Mol Pharmacol, 1996. 50(6): p. 1635-42.
34. Gao ZG, Kim SK, Gross AS, et al., *Identification of essential residues involved in the allosteric modulation of the human A_3 adenosine receptor.* Mol Pharmacol, 2003. 63(5): p. 1021-31.

35. Gao ZG, Jiang Q, Jacobson KA, et al., *Site-directed mutagenesis studies of human A_{2A} adenosine receptors: involvement of Glu^{13} and His^{278} in ligand binding and sodium modulation.* Biochem Pharmacol, 2000. 60(5): p. 661-8.
36. Shang Y, LeRouzic V, Schneider S, et al., *Mechanistic insights into the allosteric modulation of opioid receptors by sodium ions.* Biochemistry, 2014. 53(31): p. 5140-49.
37. Schetz JA and Sibley DR, *The binding-site crevice of the D_4 dopamine receptor is coupled to three distinct sites of allosteric modulation.* J Pharmacol Exp Ther, 2001. 296(2): p. 359-63.
38. Nygaard R, Frimurer TM, Holst B, et al., *Ligand binding and micro-switches in 7TM receptor structures.* Trends Pharmacol Sci, 2009. 30(5): p. 249-59.
39. Gao ZG, Chen A, Barak D, et al., *Identification by site-directed mutagenesis of residues involved in ligand recognition and activation of the human A_3 adenosine receptor.* J Biol Chem, 2002. 277(21): p. 19056-63.
40. Jiang Q, Van Rhee AM, Kim J, et al., *Hydrophilic side chains in the third and seventh transmembrane helical domains of human A_{2A} adenosine receptors are required for ligand recognition.* Mol Pharmacol, 1996. 50(3): p. 512-21.
41. Urizar E, Claeysen S, Deupí X, et al., *An activation switch in the rhodopsin family of G protein-coupled receptors: the thyrotropin receptor.* J Biol Chem, 2005. 280(17): p. 17135-41.
42. Bakker RA, Jongejan A, Sansuk K, et al., *Constitutively active mutants of the histamine H_1 receptor suggest a conserved hydrophobic asparagine-cage that constrains the activation of class A G protein-coupled receptors.* Mol Pharmacol, 2008. 73(1): p. 94-103.
43. Lebon G, Warne T, Edwards PC, et al., *Agonist-bound adenosine A_{2A} receptor structures reveal common features of GPCR activation.* Nature, 2011. 474(7352): p. 521-25.
44. Dawson ES and Wells JN, *Determination of amino acid residues that are accessible from the ligand binding crevice in the seventh transmembrane-spanning region of the human A_1 adenosine receptor.* Mol Pharmacol, 2001. 59(5): p. 1187-95.
45. Rosenbaum DM, Rasmussen SGF, and Kobilka BK, *The structure and function of G-protein-coupled receptors.* Nature, 2009. 459(7245): p. 356-63.